Above-threshold ionization of diatomic molecules by few-cycle laser pulses

A. Gazibegović-Busuladžić,[1] E. Hasović,[1,2] M. Busuladžić,[3] D. B. Milošević,[1,2,4,*] F. Kelkensberg,[5] W. K. Siu,[5] M. J. J. Vrakking,[2,5] F. Lépine,[6] G. Sansone,[7] M. Nisoli,[7] I. Znakovskaya,[8] and M. F. Kling[8,9,†]

[1]*Faculty of Science, University of Sarajevo, Zmaja od Bosne 35, 71000 Sarajevo, Bosnia and Herzegovina*

[2]*Max-Born-Institut, Max-Born-Str. 2a, D-12489 Berlin, Germany*

[3]*Medical Faculty, University of Sarajevo, Čekaluša 90, 71000 Sarajevo, Bosnia and Herzegovina*

[4]*Academy of Sciences and Arts of Bosnia and Herzegovina Bistrik 7, 71000 Sarajevo, Bosnia and Herzegovina*

[5]*FOM-Institute AMOLF, Science park 104, NL-1098 XG Amsterdam, The Netherlands*

[6]*Université Lyon 1; CNRS; LASIM, UMR 5579, 43 bvd. du 11 novembre 1918, F-69622 Villeurbanne, France*

[7]*Politecnico di Milano, Department of Physics, National Research Council of Italy, Institute of Photonics and Nanotechnologies (CNR-IFN), Piazza L. da Vinci 32, I-20133, Milano, Italy*

[8]*Max-Planck-Institut für Quantenoptik, Hans-Kopfermann-Str. 1, D-85748 Garching, Germany*

[9]*J.R. Macdonald Laboratory, Kansas State University, Manhattan, Kansas 66506, USA*

(Received 30 June 2011; published 24 October 2011)

Above-threshold ionization of diatomic molecules by infrared carrier-envelope phase (CEP) stable few-cycle laser pulses is analyzed both experimentally and theoretically. The theoretical approach is based on the recently developed molecular improved strong-field approximation (ISFA), generalized to few-cycle pulses. Instead of using the first Born approximation, the rescattering matrix element in the ISFA is now calculated exactly. This modification leads to the appearance of characteristic minima in the differential cross section as a function of the scattering angle. Experimental angle-resolved photoelectron spectra of N_2 and O_2 molecules are obtained using the velocity map imaging technique. A relatively good agreement of experimental and simulated angle-resolved spectra, CEP-dependent asymmetry maps, and extracted electron-molecular ion elastic scattering differential cross sections is obtained.

DOI: 10.1103/PhysRevA.84.043426 PACS number(s): 33.80.Rv, 32.80.Rm, 42.50.Hz

I. INTRODUCTION

Above-threshold ionization (ATI) is a process in which more photons are absorbed from a laser field than is necessary for ionization [1]. It has been found that the ionization dynamics of atoms is mainly determined by the atomic binding energy and the laser parameters [2,3]. In particular, the study of ATI by strong ultrashort few-cycle laser pulses gave an insight into this dynamics on the subfemtosecond scale [4] and stimulated the development of attoscience [5]. ATI of molecules by a strong laser field has attracted a lot of attention in recent years [6–8]. In comparison with atoms, molecules have additional features such as orbital symmetry, molecular orientation (with respect to the laser polarization axis), internuclear distance, etc., which determine the photoionization dynamics. As a consequence, the photoelectron energy- and angle-resolved spectra can be used to reveal the structure of a molecule. In particular, homonuclear diatomic molecules have two identical centers from which the electron can be ionized so that the two-center interference can be observed in the photoelectron spectra [9]. If the ionized electron, driven by the laser field, returns to the parent core, it may rescatter off it. Such a process is called high-order ATI (HATI) and it was proposed [10] to use HATI-based laser-induced electron diffraction (LIED) to extract information about the target (see also Ref. [11]). In fact, for diatomic molecules the rescattering may happen on either of the atomic centers, leading to a new type of two-source double-slit interference, as has been established recently [12]. For more recent results about LIED; see [13–19].

In [13] the observed photoelectron spectra of aligned N_2 and O_2 molecules were analyzed using a simplified plane-wave approximation. Cornaggia [14] has extracted the electron-molecular-ion differential scattering cross sections (DCSs) from his experimental data for various molecules, using the method reviewed in [8] (see also the theoretical paper [16], where it was demonstrated that it is possible to use intense infrared and midinfrared lasers to probe the structure of a molecule). Finally, in [19] the electron-ion DCSs for partially aligned O_2^+ and CO_2^+ molecules were extracted by LIED spectroscopy. In all these references the laser pulses used were long enough so that the few-cycle-pulse effects are negligible.

In the present work we will analyze, both experimentally and theoretically, the angle- and energy-resolved HATI spectra of diatomic molecules generated by infrared few-cycle laser pulses. Theoretically, we will go beyond the plane-wave approximation. Similarly as in Ref. [19], we extract the DCSs from the angle-resolved photoelectron spectra. In addition to the O_2 molecule, considered in [19], we analyze spectra of the N_2 molecule, which has a different symmetry. We will also analyze carrier-envelope phase (CEP) effects on the photoelectron spectra and discuss corresponding CEP-dependent asymmetry maps for the directional electron emission.

II. THEORY

A. Modified molecular strong-field approximation for few-cycle laser pulses

In Refs [12,20] we simulated experiments in which the HATI of nonaligned diatomic molecules N_2 and O_2 was achieved by a strong (intensity $\sim 10^{14}$ W/cm^2) laser pulse (width $\sim$100 fs). For this purpose we used our modified

*milo@bih.net.ba

†matthias.kling@mpq.mpg.de

molecular strong-field approximation (SFA) developed in Ref. [21] (see also [22] for a comparison with a different experiment) and generalized to include the rescattering effects in [23]. We have also developed a method for averaging over the spacetime distribution of the laser intensity in the focus [24,25] and for averaging over the molecular orientations [26].

In order to simulate an analogous HATI experiment in which much shorter laser pulses of about 6 fs duration were used, we have generalized our program to few-cycle laser pulses. This modification is similar to the improved SFA developed for atomic systems (see review article [4]). The focal averaging method is also modified in comparison with that of Refs. [24,25]. The time dependence of the pulse envelope is included in the calculation of the ionization probability using an electric field vector amplitude of the form

$$E(t) = E_0 \sin^2(\pi t/T_\mathrm{p}) \cos(\omega t + \varphi_\mathrm{CEP}), \tag{1}$$

where $T_\mathrm{p} = n_\mathrm{p} T = 2\pi n_\mathrm{p}/\omega$ is the total pulse duration with the number of cycles n_p and φ_CEP is the carrier-envelope phase. For spatial focal averaging we use the weak focusing approximation (where only radial variations of the laser intensity are considered) and choose $z = 0$. This assumption is well justified under the experimental conditions (see below), where the confocal parameter exceeds the interaction length by ca. 2 orders of magnitude. The electron yield, averaged over this spatial focal distribution, is then

$$\langle w_\mathbf{p} \rangle = \int_0^\infty w_\mathbf{p}(I_{\rho,\,\mathrm{max}}) \rho d\rho, \tag{2}$$

where $w_\mathbf{p}(I_{\rho,\,\mathrm{max}})$ is the differential ionization probability for detection of the electron with momentum $\mathbf{p}$, calculated at the fixed maximum intensity $I_{\rho,\,\mathrm{max}} = I_\mathrm{max} \exp(-2\rho^2/w_0^2)$ at the place ρ (fixed radial coordinate) in the focal plane (w_0 is the minimum beam waist).

Energy- and angle-resolved spectra are calculated as a function of the photoelectron energy $E_\mathbf{p} = p^2/2$ and the angle θ_e, which is the electron emission angle with respect to the laser polarization axis, so that $\langle w_\mathbf{p} \rangle = \langle w_p(\theta_\mathrm{e}) \rangle$. For a constant CEP, the asymmetry parameter $A(\varphi_\mathrm{CEP})$ is defined by [27]

$$A(\varphi_\mathrm{CEP}) = \frac{w_p(0^\circ) - w_p(180^\circ)}{w_p(0^\circ) + w_p(180^\circ)}. \tag{3}$$

B. Molecular high-order above-threshold ionization beyond the first Born approximation

The method described in the previous section takes into account the rescattering of the ionized electron off the parent molecular centers within the first Born approximation (1BA). It can be shown that, for a neutral diatomic molecule, the continuum-continuum matrix element with the two-center rescattering potential (see Eq. (17) in the second reference in [23]), within the modified molecular improved strong-field approximation (MISFA), is proportional to

$$\sum_{c=\pm 1} e^{-ic(\mathbf{k}_s - \tilde{\mathbf{p}})\cdot\mathbf{R}/2} f_c^\mathrm{1BA}(p_s,\theta_s), \tag{4}$$

where $\mathbf{R}$ is the relative nuclear coordinate, the sum is over the molecular centers A ($c = +1$) and B ($c = -1$), and the elastic electron-atomic center scattering amplitude in the 1BA is

$$f_c^\mathrm{1BA}(p_s,\theta_s) = -(2\pi)^2 \langle \tilde{\mathbf{p}} + \mathbf{A}_s | V_c(\mathbf{r}) | \mathbf{k}_s + \mathbf{A}_s \rangle, \tag{5}$$

with

$$\tilde{\mathbf{p}} = \mathbf{p} - \mathbf{A}(T_\mathrm{p}), \quad A(T_\mathrm{p}) = \frac{A_0 \sin\varphi_\mathrm{CEP}}{2\left(n_\mathrm{p}^2 - 1\right)}. \tag{6}$$

Having $\tilde{\mathbf{p}}$ in the transition amplitude, we ensure that the final state corresponds to an electron with momentum $\mathbf{p}$ at the detector outside the laser field. Both the momentum $\tilde{\mathbf{p}}$ and the stationary electron momentum $\mathbf{k}_s$ are shifted by the vector potential $\mathbf{A}_s \equiv \mathbf{A}(\tau_s)$ of the laser field at the time of rescattering τ_s. The momentum $\mathbf{k}_s$ is parallel to the laser field direction (see [4] for details).

For a description of the electron-atom scattering we use the independent-particle model potential introduced by Green *et al.* [28]. We neglect the polarization and exchange potentials and use only the static potential represented by the double-Yukawa function [29]. For the scattering of the electron off the nitrogen or oxygen atomic centers we use a potential of the form [30]

$$V_\mathrm{atom}(r) = -\frac{Z}{H}\frac{e^{-r/D}}{r}[1 + (H-1)e^{-Hr/D}], \tag{7}$$

with $H = DZ^{0.4}$ and $Z = 7$, $D = 0.776$ (for N) or $Z = 8$, $D = 0.708$ (for O). The independent-particle model was also applied to molecules in [31] (see also more recent work [32]).

The theoretical consideration of an electron-molecule collision is a difficult task. For a review of different theoretical methods see, for example, Ref. [33]. The use of the first Born approximation is justified only for high-energy electrons (hundreds of electronvolts). For impact energies from the ionization potential to ten times the ionization potential, the computation of electron-molecule scattering cross sections is most difficult. Improvement of the above-described method can be done by replacing the amplitude f_c^1BA with the exact scattering amplitude

$$f_c(p_s,\theta_s) = -(2\pi)^2 \langle \psi_{\tilde{\mathbf{p}}+\mathbf{A}_s} | V_c(\mathbf{r}) | \mathbf{k}_s + \mathbf{A}_s \rangle, \tag{8}$$

as it was done in Refs [34–36]. We called this method the low-frequency approximation (LFA) in analogy with the LFA for laser-assisted electron-atom scattering introduced by Kroll and Watson [37] to improve the treatment of laser-assisted potential scattering in the 1BA given in [38]. In the present context we will use the so-called on-shell LFA [39] (see also [40] for the off-shell LFA), in which the matrix element is calculated on the energy shell; namely,

$$E_s = \frac{\mathbf{p}_s^2}{2} = \frac{1}{2}(\tilde{\mathbf{p}} + \mathbf{A}_s)^2 = \frac{1}{2}(\mathbf{k}_s + \mathbf{A}_s)^2. \tag{9}$$

If, instead of the scattering amplitude, we use the square root of the DCS calculated for the energy which corresponds to the cutoff of the HATI spectrum, then our approach is equivalent to the so-called quantitative rescattering (QRS) theory (see [8] and references therein). For the calculations of the exact scattering amplitude we use the method of Ref. [41] as described in [34].

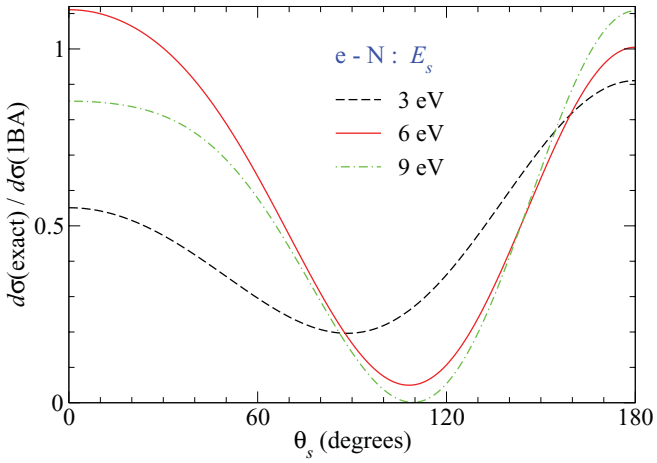

FIG. 1. (Color online) Ratios of exact and 1BA differential cross sections for elastic electron-nitrogen atom scattering as functions of the scattering angle for the fixed electron energies denoted in the legends.

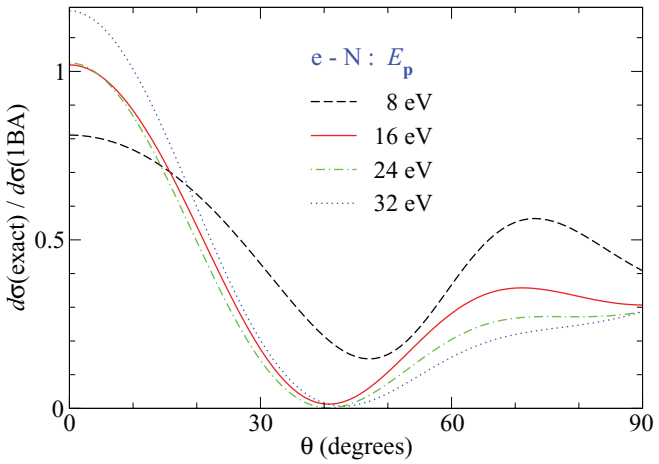

FIG. 2. (Color online) Ratios of exact and 1BA differential cross sections for elastic scattering of electrons off N atoms as functions of the angle θ for the various fixed electron energies $E_{\mathbf{p}}$ denoted in the legends. The connection between the energies $E_{\mathbf{p}}$ and the angles θ of the electron detected in HATI experiments and the scattering energies E_s and the angles θ_s is given in the text.

In Fig. 1 we present the ratio of the DCSs calculated using the exact scattering amplitude with that calculated using the 1BA; that is,

$$\frac{d\sigma(\text{exact})}{d\sigma(\text{1BA})} = \frac{|f_c(p_s,\theta_s)|^2}{\left|f_c^{\text{1BA}}(p_s,\theta_s)\right|^2}, \tag{10}$$

as a function of the scattering angle θ_s for a few energies E_s relevant to the experiment. The maximum energy at the time of rescattering is $3.173U_{\text{P}}$, where $U_{\text{P}} = I/(4\omega^2)$ is the electron's ponderomotive energy in the laser field, I is the laser intensity, and ω is the angular frequency. The wavelength used is 750 nm, the intensity is 4.3×10^{13} W/cm^2, and the total pulse duration is 6 optical cycles [6 fs full width at half maximum (FWHM)] for N_2, similar to the experimental parameters (see below). This corresponds to $E_{\text{max},s} = 7.166$ eV. In Fig. 1 we see that, for the electron-nitrogen atom scattering there are pronounced minima in the ratio [Eq. (10)] for the angles θ_s between 88° (for $E_s = 3$ eV) and 109° (for $E_s = 9$ eV). The appearance of these minima is the main modification introduced by the LFA or QRS theory.

In order to see how the minima shown in Fig. 1 show up in HATI spectra, we should relate E_s and θ_s with the energies $E_{\mathbf{p}}$ and the angles θ of the electrons detected in a HATI experiment. The final (drift) electron momentum at the detector is $\mathbf{p} = (p_z, p_x) = (p\cos\theta, p\sin\theta)$, while the electron momentum immediately after the rescattering is $\mathbf{p}_s = (p_s\cos\varphi, p_s\sin\varphi)$. The angles θ and φ are defined in the laboratory system. Using the relation $\tilde{\mathbf{p}} + \mathbf{A}_s = \mathbf{p}_s$, we obtain

$$\tan\varphi = \frac{p\sin\theta}{\tilde{p}_z + A_s}, \quad \tilde{p}_z = p\cos\theta - A(T_{\text{p}}). \tag{11}$$

The scattering angle θ_s is defined in the scattering system whose z axis is defined by the vector $\mathbf{k}_s + \mathbf{A}_s$. For a linearly polarized laser field in the z direction and for the dominant quantum orbits [42], we have $k_s + A_s < 0$ and $\theta_s = \varphi - \pi$; see Fig. 1 in [34].

It was shown in [8,34] that, for an arbitrary angle θ, the ratio p_s/A_s is approximately constant and equal to $-a = -\sqrt{3.173/2}$. Using this and solving the equation $\mathbf{p}_s^2 - (\tilde{\mathbf{p}} + \mathbf{A}_s)^2 = 0$ over p_s, we obtain $p_s = a|A_s|$, with

$$A_s = \frac{1}{a^2-1}[\tilde{p}_z - \text{sgn}(\tilde{p}_z)\sqrt{a^2\tilde{\mathbf{p}}^2 - p^2\sin^2\theta}]. \tag{12}$$

For fixed $E_{\mathbf{p}} = \mathbf{p}^2/2$, θ, and $A(T_{\text{p}})$, and by using Eqs. (11) and (12), we first calculate E_s and θ_s and then the corresponding DCSs using the method of Refs [34,41].

The results obtained using the above-described method for $\varphi_{\text{CEP}} = 0$ are shown in Fig. 2. For N atoms the minima appear at the angles θ between 47° (for $E_{\mathbf{p}} = 8$ eV) and $\theta = 41°$ (for 16 eV and for 24 eV).

We have also performed an analysis of the CEP-dependence of the ratio of the exact and 1BA DCSs for electron-nitrogen elastic scattering. We fixed the energy to $E_{\mathbf{p}} = 20$ eV and chose the laser parameters as before. Since the laser intensity used in the experiment is relatively low, the shift of the momentum $\mathbf{p}$ for $\mathbf{A}(T_{\text{p}})$ is small (less than 1%), so that the obtained position of the minimum at $\theta_{\text{min}} = 40°$ does not change with φ_{CEP}. For shorter pulses, stronger fields, and lower electron energies, the shift of the angle θ_{min} with the change of φ_{CEP} can be up to a few degrees.

We have obtained similar results for the electron-oxygen atom scattering. In this respect, the experimental spectra of N_2 and O_2 should be similar. We expect that the main difference between these spectra should be caused by different symmetries of the ground-state wave function.

In our theoretical method we neglected Coulomb effects. Since it is known that these effects modify low-energy spectra of electrons which are not rescattered [4], our results are less applicable for electrons with energies below $3U_{\text{P}}$. The Coulomb potential $-1/r$ is also important for small scattering angles. However, for HATI spectra, the electrons are backscattered near the atomic core where the potential is much larger than the $-1/r$ potential. Therefore, we expect

that the difference in DCS between neutral and singly charged molecular ions is negligible for these rescattered electrons. Finally, it should be mentioned that more realistic potentials than our double-Yukawa potential (7) can be used [32], but we do not expect that the use of such potentials will introduce any substantial change in our results.

III. COMPARISON OF THE THEORY AND EXPERIMENT

A. Experiment

In the experiments, linearly polarized, CEP-stabilized infrared few-cycle laser pulses at a central wavelength of 750 nm were obtained from a Ti:sapphire laser system operating at a 1 kHz repetition rate (see [43] for details). The pulse duration was 6 fs FWHM, corresponding to ca. 6 cycles [when applying Eq. (1) to describe the field]. The pulses were focused into the center of the ion optics of a velocity map imaging (VMI) spectrometer [44] with a spherical mirror ($f = 32$ cm). Photoelectrons generated at the crossing point of the laser and an effusive gas jet, which restricted the interaction to a length of ca. 200 μm, were projected by the ion optics onto a microchannel plate (MCP) phosphor screen assembly and recorded by a CCD camera. The three-dimensional (3D) momentum distributions of the photoelectrons were reconstructed from the recorded projections by applying an iterative inversion procedure [45]. Intensities of 4.3×10^{13} W/cm^2 for N_2 and 4.0×10^{13} W/cm^2 for O_2 were determined from the cutoff energies in the experimental photoelectron spectra (with an uncertainty of about 20%) and verified by comparison to calculated cutoff values.

In the experiments, the CEP is shifted by the insertion of dispersive material into the beam path using fused silica wedges. The experimental data are measured as a function of a relative phase, which exhibits an offset with respect to the absolute phase. The phase offset was determined by comparing the experimental data with the theoretical asymmetry data at high electron kinetic energies near the cutoff of the spectra and has already been corrected for in the data presented below.

B. Angle-resolved photoelectron spectra

In this section we compare the experimental (upper panels) and theoretical (lower panels) angle-resolved photoelectron spectra obtained by photoionization of randomly oriented N_2 (Fig. 3) and O_2 (Fig. 4) molecules. We used the experimental parameters in the calculations.

Similarly to the case of photoionization of atoms [27], the spectra of both N_2 and O_2 molecules exhibit an asymmetry for photoemission in the directions $\theta_e = 0^\circ$ and $\theta_e = 180^\circ$. This feature is well explained in the literature (see, for example, [4]). In addition to this, both the experimental and the theoretical spectra are characterized by the minima for energies in the interval 10–14 eV and for emission angles around -45°, 45°, 135°, and 225°. Such minima, denoted by arrows in Figs. 3 and 4, do not appear if we use our earlier MISFA theory. This confirms that one should use the exact scattering amplitude (i.e., molecular LFA theory) described in Sec. II B.

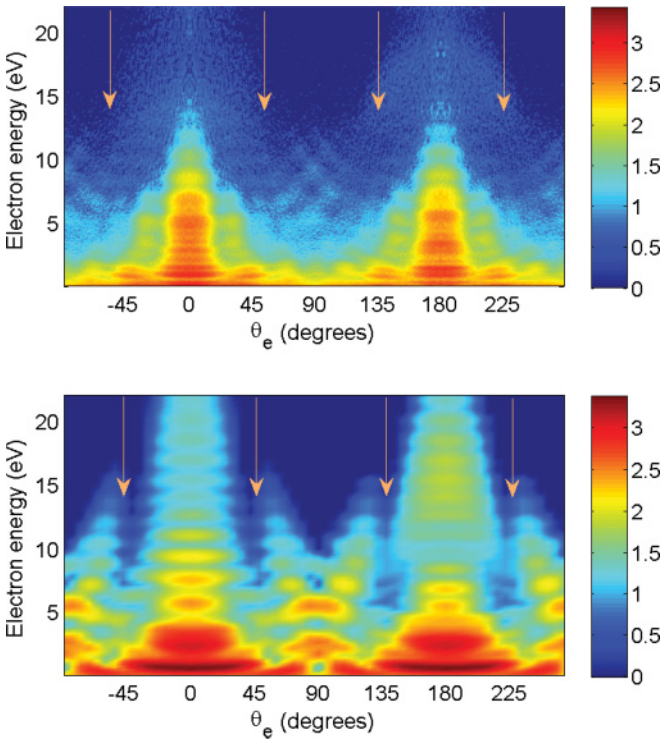

FIG. 3. (Color online) Comparison of experimental (upper panel) with theoretical (lower panel) angle-resolved photoelectron spectra of randomly oriented N_2 molecules ionized by an ultrashort (pulse duration 6 optical cycles) CEP-stabilized ($\varphi_{CEP} = 0$) laser pulse with a wavelength of 750 nm and a peak intensity of 4.3×10^{13} W/cm^2. On the abscissa the electron emission angle with respect to the laser polarization axis is denoted, while the photoelectron energy in electronvolts is shown on the ordinate. The same colorbar which covers 3.4 orders of magnitude is used in both panels. The arrows point toward the minima.

Comparing the theoretical with the experimental angle-resolved spectra for N_2 and O_2 (Figs. 3 and 4) for θ_e around -90° and 90° and for electron energies in the interval 5–10 eV, one can notice that the theoretical spectra reproduce the structure of the experimental spectra, but that the corresponding ionization probability is slightly overestimated.

The difference between the N_2 and O_2 spectra caused by different symmetries of the ground-state wave functions is clearly visible in the case of aligned molecules [23]. For random molecular orientation, after averaging over the molecular orientation, this difference manifests as a slightly lower high-energy plateau for O_2 due to the π_g symmetry of its ground-state wave function. This was experimentally observed [12] and is also visible in the calculations.

C. Asymmetry maps

In Figs. 5 and 6 we compare the asymmetries [Eq. (3)], calculated using the experimental and theoretical data. Experimental data for the emission angle in Eq. (3) were averaged over a bin size of 30° ($\pm 15^\circ$) to get more reliable results. For the N_2 molecule (Fig. 5) there is a good qualitative agreement between the theoretical and experimental asymmetries. For

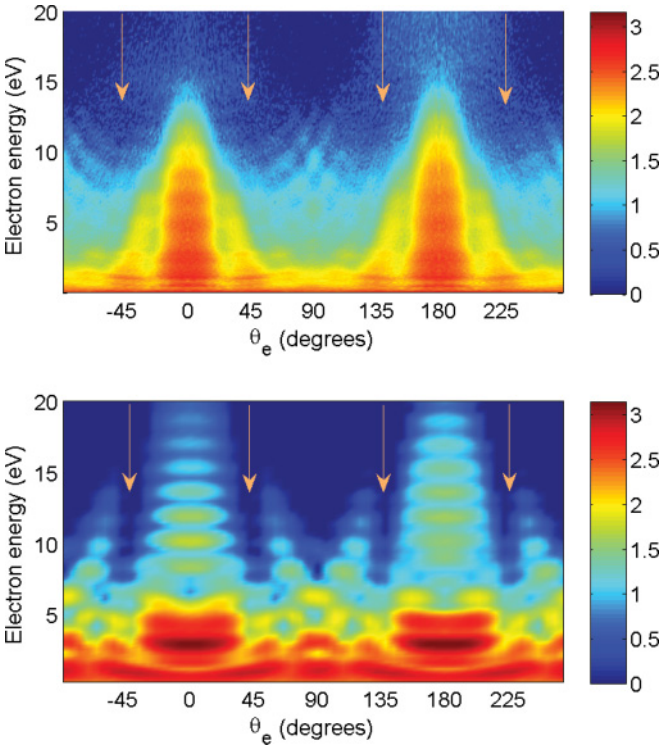

FIG. 4. (Color online) Same as in Fig. 3, but for O_2 molecules and for the peak intensity 4.0×10^{13} W/cm^2. The colorbar covers 3.2 orders of magnitude.

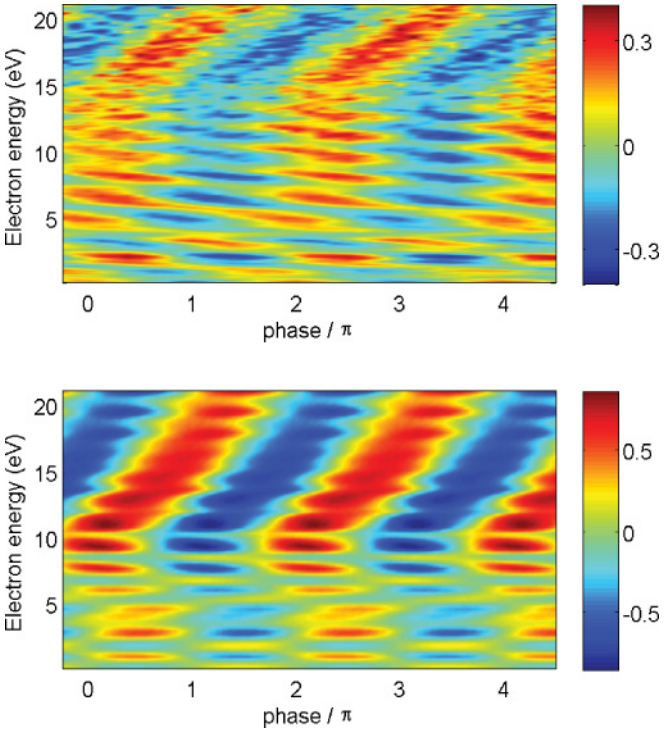

FIG. 5. (Color online) Comparison of experimental (upper panel) with theoretical (lower panel) asymmetries (expressed using false colors with the corresponding colorbar), for randomly oriented N_2 molecules. Asymmetries are presented as a function of the phase φ_{CEP} (abscissa) and the electron energy in electronvolts (ordinate). Laser pulse parameters are as in Fig. 3.

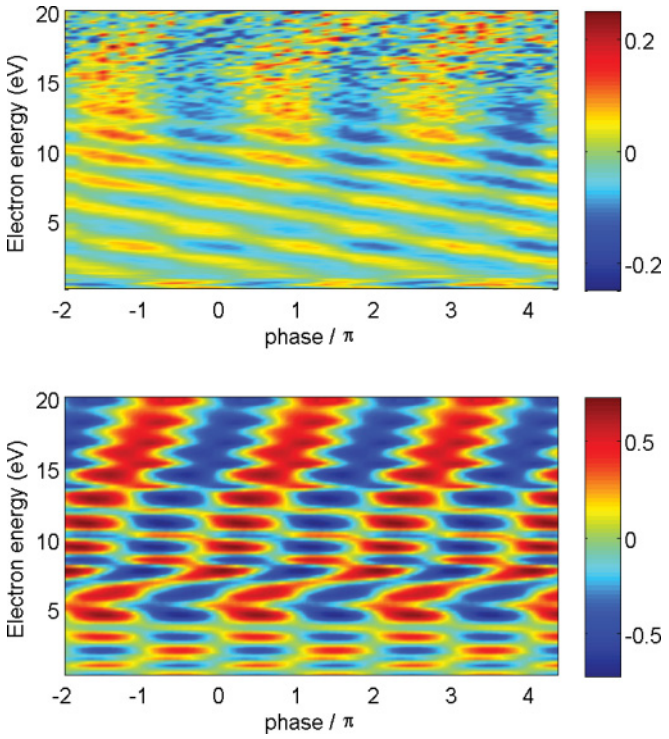

FIG. 6. (Color online) Same as in Fig. 5, but for the O_2 molecule and with laser pulse parameters as for Fig. 4.

example, there is a very similar asymmetry inclination in the photoelectron energy range 13–21 eV (for the O_2 molecule the corresponding range is 15–20 eV). Similarly as for HATI of atoms, this asymmetry inclination can be explained as the CEP and photoelectron-energy-dependent interference of a few saddle-point solutions [46]. It is interesting that this interference has survived focal and orientation averaging. The quantitative agreement between the theoretical and experimental asymmetries is not that good, possibly due to the influence of background in the higher-energy part of the experimental spectra, which also reduces the strength of the experimentally determined asymmetry.

The kink at 10 eV in the theoretical asymmetries is connected with the transition from the region where the main contribution to the spectra comes from directly emitted photoelectrons to the energy region where only the rescattered electrons contribute. Since we have neglected Coulomb effects which modify the direct spectra [4], we expect that this kink should appear at larger energies. And in agreement with this expectation, in the experimental asymmetries, this kink appears slightly below 15 eV.

It is interesting that the theoretical asymmetry plots obtained within the MISFA are almost the same as those obtained within the modified molecular on-shell LFA. This can be explained using the results presented in Fig. 1: the ratio of the exact and the 1BA DCSs for backscattering is close to 1.

In comparison with the spectra of the N_2 molecule, the direct ATI spectra of the O_2 molecule are suppressed for low energies due to a different symmetry of the corresponding ground-state wave function. However, since the asymmetry parameter (3) is defined as the ratio of the yields, this suppression is not noticeable in the asymmetry plots. As we

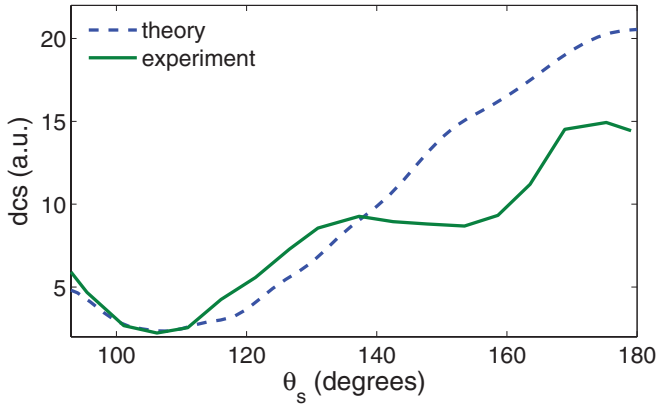

FIG. 7. (Color online) Comparison of angular distributions of elastic differential cross sections for electron-scattering energy of 5.6 eV, extracted from experimental and from theoretical CEP-averaged photoelectron spectra for N_2, with laser pulse parameters as for Fig. 3, and random molecular orientation. The position of the minima of theoretical and experimental DCSs agree well.

have mentioned, the rescattering spectra for N_2 and O_2 are similar and so are the corresponding asymmetry plots.

D. Differential cross sections

A comparison of the large-angle elastic DCSs for electron-molecular positive ion elastic scattering, extracted from the experimental and the theoretical photoelectron spectra of N_2 and O_2 molecules in an ultrashort infrared laser field, is presented in Figs. 7 and 8. As the experiments were conducted at relatively low laser intensities, the signal-to-noise ratio for electron energies at about $10U_P$ was not suited for extracting reliable DCSs. The advantage of extracting DCSs from spectra for ultrashort laser pulses is that the factorization formula [19], according to which $\langle w_{\mathbf{p}} \rangle \propto$ DCS, holds for a wider range of photoelectron energies within the rescattering plateau. The reason for this is that a smaller number of quantum orbits contributes to the plateau [4,34,42]. Therefore, for the short pulses used here, the comparison of the DCSs can be attempted for lower electron energies.

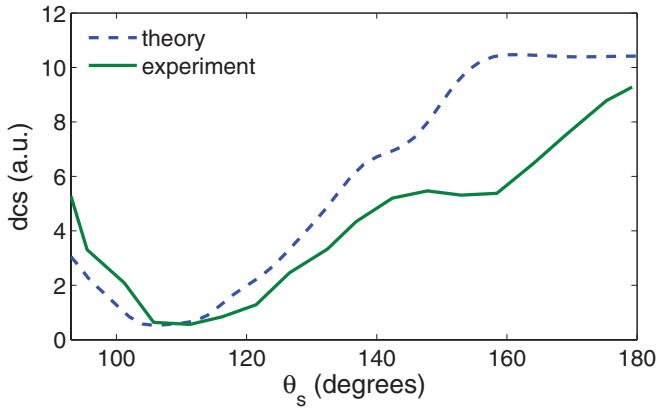

FIG. 8. (Color online) Same as in Fig. 7, but for O_2 molecules, for electron scattering energy of 6 eV and with laser pulse parameters as for Fig. 4.

According to the theory presented in Sec. II B, the minima in HATI spectra for angles $\theta = \theta_e$ near 40° to 45° (see Fig. 2) are related to the minima in the DCSs at 100° to 110° (see Fig. 1). Since our angle-resolved HATI spectra, shown in Figs. 3 and 4, exhibit minima at 45° we expect to have minima in the DCSs at 110°. The explicit procedure of extracting this information from the spectra is the following: For photoelectrons registered at the detector with momentum $\mathbf{p} = \tilde{\mathbf{p}} + \mathbf{A}(T_p)$, after being backscattered in such a way that $\tilde{\mathbf{p}} = -\mathbf{A}_s + \mathbf{p}_s$, the relation $p_s = a|A_s|$ is a good approximation. For ultrashort pulses the factorization formula can be applied if the electron kinetic energy $\mathbf{p}^2/2$ is $4U_P$ or higher. The corresponding elastic DCS for scattering energy $\mathbf{p}_s^2/2$ can be extracted from a semicircle of radius p_s centered at $p_z = A_s$, $p_x = 0$ in the two-dimensional momentum plane. In order to obtain proper quantitative and qualitative values of the DCSs for $\theta_s > 90°$, we calculated the actual flux of the returning electron wave packet and averaged over CEPs and molecular orientations. Elastic DCSs extracted from theoretical HATI spectra are scaled with such calculated fluxes. This procedure is justified with the findings that the flux of the returning electron wave packet with the momentum near p_s depends very weakly on θ_s for $\theta_s > 120°$ (see [8] and references therein).

Here we present the elastic DCSs for electron scattering energies of 5.6 eV for N_2 (Fig. 7) and of 6 eV for O_2 (Fig. 8), extracted from the experimental and theoretical spectra. The first energy corresponds to the registered photoelectron energy of $4.45U_P$ (10 eV), while the second one corresponds to $5.6U_P$ (11.8 eV) for $\theta_e = 0°$. To smooth out the ATI peaks, both the theoretical and the experimental DSCs are obtained by averaging the data over bins of $\Delta p_s = 0.08$ a.u. and $\Delta\theta_s = 6°$.

The agreement between the theoretical and experimental results is good. In particular, there are pronounced minima at $\theta_s \approx 110°$ in the extracted DCSs both for N_2 and O_2.

IV. CONCLUSIONS

In this work we have presented a comparison of experimental and theoretical results for angle- and energy-resolved photoelectron spectra of diatomic molecules (exemplified by N_2 and O_2 molecules) ionized by infrared few-cycle laser pulses. For the ultrashort laser pulses used in the present study, the left-right (i.e., $\theta_e = 0°$ vs $\theta_e = 180°$) asymmetry, well known from the stereo-HATI experiments with stabilized CEP [47] for atoms, was also observed in the molecular case.

A relatively good agreement between theoretical and experimental results was obtained by modifying our improved molecular strong-field approximation. We have developed a so-called LFA theory in which the scattering amplitude, calculated in the first Born approximation in the MISFA theory, is replaced by the exact scattering amplitude. As a consequence, minima near $45° + k \times 90°$, $k = 0, \pm 1, 2$, have appeared in the calculated spectra, which is in agreement with the experimental results.

Furthermore, we were able to extract the differential elastic scattering cross section both from the experimental and from the theoretical results. Taking into account that the experimental signal-to-noise ratio was low for high-energy electrons, the agreement of our theoretical results with experimental results is reasonably good. In particular, the position of minima at particular values of θ_s in the extracted DCSs is the same. It should also be mentioned that the theoretical spectrum was calculated within the on-shell LFA theory in which Coulomb effects are not taken into account, so that a reasonable agreement with experiment is expected to be found only in the high-energy part of the spectrum (for the photoelectron energies above $3U_P$, which is above 7 eV for the laser pulse parameters used herein).

We have also compared theoretical and experimental asymmetry plots. As in the atomic case [27], the agreement is relatively good.

ACKNOWLEDGMENTS

Sponsorship has been provided by the Alexander von Humboldt Foundation and funding by the German Federal Ministry of Education and Research in the framework of the Research Group Linkage Programme. We acknowledge support by the Max Planck Society, the European network ATTOFEL, Laserlab Europe, the German Science Foundation via the Emmy-Noether program, and the Cluster of Excellence: Munich Center for Advanced Photonics and the "Stichting voor Fundamenteel Onderzoek der Materie" (FOM), which is financially supported by the "Nederlandse Organisatie voor Wetenschappelijk Onderzoek" (NWO). We are grateful for support from the Chemical Sciences, Geosciences, and Biosciences Division, Office of Basic Energy Sciences, Office of Science, US Department of Energy.

[1] P. Agostini, F. Fabre, G. Mainfray, G. Petite, and N. K. Rahman, Phys. Rev. Lett. **42**, 1127 (1979).
[2] L. F. DiMauro and P. Agostini, Adv. At. Mol. Opt. Phys. **35**, 79 (1995).
[3] W. Becker, F. Grasbon, R. Kopold, D. B. Milošević, G. G. Paulus, and H. Walther, Adv. At. Mol. Opt. Phys. **48**, 35 (2002).
[4] D. B. Milošević, G. G. Paulus, D. Bauer, and W. Becker, J. Phys. B **39**, R203 (2006).
[5] F. Krausz and M. Ivanov, Rev. Mod. Phys. **81**, 163 (2009).
[6] A. Becker and F. H. M. Faisal, J. Phys. B **38**, R1 (2005).
[7] M. Lein, J. Phys. B **40**, R135 (2007).
[8] C. D. Lin, A.-T. Le, Z. Chen, T. Morishita, and R. Lucchese, J. Phys. B **43**, 122001 (2010).
[9] H. D. Cohen and U. Fano, Phys. Rev. **150**, 30 (1966). For more recent work see, for example: Z. Ansari, M. Böttcher, B. Manschwetus, H. Rottke, W. Sandner, A. Verhoef, M. Lezius, G. G. Paulus, A. Saenz, and D. B. Milošević, New J. Phys. **10**, 093027 (2008); A. Picón, A. Bahabad, H. C. Kapteyn, M. M. Murnane, and A. Becker, Phys. Rev. A **83**, 013414 (2011), and references therein. New features in double-slit-like interference for higher photon energies have been investigated recently in: S. X. Hu, L. A. Collins, and B. I. Schneider, *ibid.* **80**, 023426 (2009), and commented in: M. J. J. Vrakking, Physics **2**, 72 (2009).
[10] T. Zuo, A. D. Bandrauk, and P. B. Corkum, Chem. Phys. Lett. **259**, 313 (1996).
[11] M. Spanner, O. Smirnova, P. B. Corkum, and M. Yu. Ivanov, J. Phys. B **37**, L243 (2004); S. N. Yurchenko, S. Patchkovskii, I. V. Litvinyuk, P. B. Corkum, and G. L. Yudin, Phys. Rev. Lett. **93**, 223003 (2004).
[12] M. Okunishi, R. Itaya, K. Shimada, G. Prümper, K. Ueda, M. Busuladžić, A. Gazibegović-Busuladžić, D. B. Milošević, and W. Becker, Phys. Rev. Lett. **103**, 043001 (2009).
[13] M. Meckel *et al.*, Science **320**, 1478 (2008).
[14] C. Cornaggia, Phys. Rev. A **78**, 041401 (2008); J. Phys. B **42**, 161002 (2009); Phys. Rev. A **82**, 053410 (2010).
[15] H. Kang *et al.*, Phys. Rev. Lett. **104**, 203001 (2010).
[16] J. Xu, Z. Chen, A.-T. Le, and C. D. Lin, Phys. Rev. A **82**, 033403 (2010).
[17] B. Wang, Y. Guo, B. Zhang, Z. Zhao, Z.-C. Yan, and P. Fu, Phys. Rev. A **82**, 043402 (2010).
[18] Y. Huismans *et al.*, Science **331**, 61 (2011).
[19] M. Okunishi, H. Niikura, R. R. Lucchese, T. Morishita, and K. Ueda, Phys. Rev. Lett. **106**, 063001 (2011).
[20] M. Okunishi, R. Itaya, K. Shimada, G. Prümper, K. Ueda, M. Busuladžić, A. Gazibegović-Busuladžić, D. B. Milošević, and W. Becker, J. Phys. B **41**, 201004 (2008).
[21] D. B. Milošević, Phys. Rev. A **74**, 063404 (2006).
[22] M. Busuladžić and D. B. Milošević, Phys. Rev. A **82**, 015401 (2010).
[23] M. Busuladžić, A. Gazibegović-Busuladžić, D. B. Milošević, and W. Becker, Phys. Rev. Lett. **100**, 203003 (2008); Phys. Rev. A **78**, 033412 (2008); M. Busuladžić, A. Gazibegović-Busuladžić, and D. B. Milošević, *ibid.* **80**, 013420 (2009); Laser Phys. **20**, 1001 (2010).
[24] R. Kopold, W. Becker, M. Kleber, and G. G. Paulus, J. Phys. B **35**, 217 (2002).
[25] D. B. Milošević, A. Gazibegović-Busuladžić, and W. Becker, Phys. Rev. A **68**, 050702(R) (2003); A. Gazibegović-Busuladžić, D. B. Milošević, and W. Becker, *ibid.* **70**, 053403 (2004); A. Gazibegović-Busuladžić, D. B. Milošević, W. Becker, B. Bergues, H. Hultgren, and I. Yu. Kiyan, Phys. Rev. Lett. **104**, 103004 (2010).
[26] D. B. Milošević, M. Busuladžić, A. Gazibegović-Busuladžić, and W. Becker, Chem. Phys. **366**, 85 (2009).
[27] M. F. Kling, J. Rauschenberger, A. J. Verhoef, E. Hasović, T. Uphues, D. B. Milošević, H. G. Muller, and M. J. J. Vrakking, New J. Phys. **10**, 025024 (2008).
[28] A. E. S. Green, D. L. Sellin, and A. S. Zachor, Phys. Rev. **184**, 1 (1969).
[29] A. E. S. Green, D. E. Rio, and T. Ueda, Phys. Rev. A **24**, 3010 (1981).
[30] A. Čerkić and D. B. Milošević, Phys. Rev. A **70**, 053402 (2004); A. Čerkić and D. B. Milošević, Laser Phys. **15**, 268 (2005).
[31] T. Sawada, P. S. Ganas, and A. E. S. Green, Phys. Rev. A **9**, 1130 (1974).
[32] V. N. Glushkov, S. I. Fesenko, and A. Ya. Tsaune, Opt. Spectrosk. **98**, 902 (2005) [Opt. Spectrosc. **98**, 823 (2005)].
[33] N. F. Lane, Rev. Mod. Phys. **52**, 29 (1980).
[34] A. Čerkić, E. Hasović, D. B. Milošević, and W. Becker, Phys. Rev. A **79**, 033413 (2009).

[35] D. B. Milošević, A. Čerkić, B. Fetić, E. Hasović, and W. Becker, Laser Phys. **20**, 573 (2010).
[36] D. B. Milošević, W. Becker, M. Okunishi, G. Prümper, K. Shimada, and K. Ueda, J. Phys. B **43**, 015401 (2010).
[37] N. M. Kroll and K. M. Watson, Phys. Rev. A **8**, 804 (1973).
[38] F. V. Bunkin and M. V. Fedorov, Zh. Eksp. Teor. Fiz. **49**, 1215 (1965) [Sov. Phys. JETP **22**, 844 (1965)].
[39] P. S. Krstić and D. B. Milošević, J. Phys. B **20**, 3487 (1987); D. B. Milošević and P. S. Krstić, *ibid*. **20**, 2843 (1987); **21**, L303 (1988).
[40] D. B. Milošević, J. Phys. B **28**, 1869 (1995); Phys. Rev. A **53**, 619 (1996).
[41] *Computational Atomic Physics. Electron and Positron Collisions with Atoms and Ions*, edited by K. Bartschat (Springer, Berlin, 1996).
[42] D. B. Milošević, E. Hasović, M. Busuladžić, A. Gazibegović-Busuladžić, and W. Becker, Phys. Rev. A **76**, 053410 (2007).
[43] G. Sansone *et al*., Science **314**, 443 (2006).
[44] O. Ghafur, W. Siu, P. Johnsson, M. F. Kling, M. Drescher, and M. J. J. Vrakking, Rev. Sci. Instr. **80**, 033110 (2009).
[45] M. J. J. Vrakking, Rev. Sci. Instr. **72**, 4084 (2001).
[46] D. B. Milošević, G. G. Paulus, and W. Becker, Phys. Rev. A **71**, 061404 (2005).
[47] G. G. Paulus, F. Lindner, H. Walther, A. Baltuška, E. Goulielmakis, M. Lezius, and F. Krausz, Phys. Rev. Lett. **91**, 253004 (2003).